International Journal for Parasitology 48 (2018) 955–968

Contents lists available at ScienceDirect

International Journal for Parasitology

journal homepage: www.elsevier.com/locate/ijpara

Glycolysis is important for optimal asexual growth and formation of mature tissue cysts by *Toxoplasma gondii*

Anurag Shukla [a], Kellen L. Olszewski [b], Manuel Llinás [c], Leah M. Rommereim [d,1], Barbara A. Fox [d], David J. Bzik [d], Dong Xia [e], Jonathan Wastling [f], Daniel Beiting [g], David S. Roos [h,*], Dhanasekaran Shanmugam [a,*]

[a] *Biochemical Sciences Division, CSIR-National Chemical Laboratory, Pune, India*
[b] *Department of Metabolomics, Kadmon Corporation, New York, USA*
[c] *Department of Biochemistry and Molecular Biology and Department of Chemistry, Huck Center for Malaria Research, The Pennsylvania State University, W126 Millennium Science Complex, University Park, PA, USA*
[d] *Department of Microbiology and Immunology, Geisel School of Medicine at Dartmouth, Lebanon, NH, USA*
[e] *The Royal Veterinary College, London NW1 0TU, UK*
[f] *Faculty of Natural Sciences, Keele University, Keele, Staffordshire, ST5 5BG, UK*
[g] *School of Veterinary Medicine, Dept. of Pathobiology, University of Pennsylvania, Philadelphia, PA, USA*
[h] *Department of Biology and Penn Genome Frontiers Institute, University of Pennsylvania, Philadelphia, PA, USA*

ARTICLE INFO

Article history:
Received 20 March 2018
Received in revised form 28 May 2018
Accepted 31 May 2018
Available online 31 August 2018

Keywords:
Toxoplasma gondii
Glycolysis
Gluconeogenesis
Metabolomics
Hexokinase
ATP synthesis

ABSTRACT

Toxoplasma gondii can grow and replicate using either glucose or glutamine as the major carbon source. Here, we have studied the essentiality of glycolysis in the tachyzoite and bradyzoite stages of *T. gondii*, using transgenic parasites that lack a functional hexokinase gene (*Δhk*) in RH (Type-1) and Prugniaud (Type-II) strain parasites. Tachyzoite stage *Δhk* parasites exhibit a fitness defect similar to that reported previously for the major glucose transporter mutant, and remain virulent in mice. However, although Prugniaud strain *Δhk* tachyzoites were capable of transforming into bradyzoites in vitro, they were severely compromised in their ability to make mature bradyzoite cysts in the brain tissue of mice. Isotopic labelling studies reveal that glucose-deprived tacyzoites utilise glutamine to replenish glycolytic and pentose phosphate pathway intermediates via gluconeogenesis. Interestingly, while glutamine-deprived intracellular *Δhk* tachyzoites continued to replicate, extracellular parasites were unable to efficiently invade host cells. Further, studies on mutant tachyzoites lacking a functional phospho-enolpyruvate carboxykinase (*Δpepck1*) revealed that glutaminolysis is the sole source of gluconeogenic flux in glucose-deprived parasites. In addition, glutaminolysis is essential for sustaining oxidative phosphorylation in *Δhk* parasites, while wild type (*wt*) and *Δpepck1* parasites can obtain ATP from either glycolysis or oxidative phosphorylation. This study provides insights into the role of nutrient metabolism during asexual propagation and development of *T. gondii*, and validates the versatile nature of central carbon and energy metabolism in this parasite.

1. Introduction

Apicomplexan species are remarkably diverse in their cellular metabolism, often harbouring a reduced set of pathways in comparison to their hosts or even related free-living protists (Woo et al., 2015). As a consequence, these parasites resort to scavenging a variety of essential nutrients and metabolites from the host (Polonais and Soldati-Favre, 2010). Glucose is the preferred nutrient for *Toxoplasma gondii* and its assimilation via glycolysis supports optimal growth of the parasite. In addition, certain glycolytic enzymes are located in the apicoplast (Fleige et al., 2007), a secondary endosymbiotic plastid organelle (McFadden et al., 1996; Köhler et al., 1997), where they are involved in the interconversion of triose-phosphate intermediates to provide precursors for biosynthesis of fatty acids (acetyl-CoA) and isoprene units (pyruvate and glyceraldehyde 3-phosphate) (Roos et al., 2002; Seeber, 2003; Seeber and Soldati-Favre, 2010; Ralph et al., 2004). Moreover, the pyruvate dehydrogenase enzyme, which converts the glycolytic end product pyruvate to acetyl-CoA, is located only

* Corresponding authors.
E-mail addresses: droos@sas.upenn.edu (D.S. Roos), d.shanmugam@ncl.res.in (D. Shanmugam).
[1] Present address: Institute for Systems Biology, Seattle, WA, USA.

https://doi.org/10.1016/j.ijpara.2018.05.013
0020-7519/

in the apicoplast and hence may have no role in mitochondrial acetyl CoA production (Foth et al., 2005; Crawford et al., 2006). Instead, the branched chain keto-acid dehydrogenase (BCKDH) enzyme was shown to facilitate the synthesis of acetyl-CoA in the mitochondrion of *Toxoplasma* and *Plasmodium* (Oppenheim et al., 2014). It is also likely that pyruvate is converted to oxaloacetate by pyruvate carboxylase enzyme in the mitochondrion (MacRae et al., 2012), although the expression of this enzyme in tachyzoite stage parasites appears to be very low (Nitzsche et al., 2017). The flux of carbon from glycolysis into the Krebs cycle has been demonstrated previously in *T. gondii* by metabolic labelling studies, in both extracellular and intracellular tachyzoite stage parasites (MacRae et al., 2012). Glycolysis is also the major source of cellular ATP in *T. gondii*. Biochemical studies in *T. gondii* indicate that bulk ATP production can be accounted for by glycolysis, rather than by mitochondrial oxidative phosphorylation (Saliba and Kirk, 2001; Al-Anouti et al., 2004; Lin et al., 2011).

Despite the importance of glucose as a key nutrient, tachyzoite stage mutant parasites lacking the major glucose transporter (*Tg*gt1) were viable (Blume et al., 2009). Glutamine was found to be necessary for growth and motility of *gt1* mutant parasites (*Δgt1*), and metabolic labelling studies revealed an active gluconeogenic pathway via which carbon derived from glutaminolysis was channelled to replenish glycolytic intermediates (Nitzsche et al., 2016). The non-essentiality of glycolysis was further confirmed by the finding that the glycolytic enzyme aldolase is dispensable in tachyzoite stage *T. gondii* (Shen and Sibley, 2014). In the absence of robust glycolysis, as is the case in *Δgt1* mutants, glutamine is the key nutrient supporting the survival of the parasite (MacRae et al., 2012; Nitzsche et al., 2016). Glutaminolysis contributes carbon flux to the Krebs cycle, and helps replenish glycolytic intermediates via gluconeogenesis, thereby facilitating the growth and replication of *Δgt1* parasites. This finding was further supported by the fact that phosphoenolpyruvate carboxykinase (*pepck1*) enzyme, which catalyses the first step in glyconeogenesis is essential for survival of *T. gondii* in the absence of glycolysis (Nitzsche et al., 2017).

However, the role of glycolysis during asexual stage conversion and tissue cyst formation in animal hosts is yet to be studied. Bradyzoite stage parasites are characterised by the presence of intracellular amylopectin granules, and the cyst wall they form contains lectin binding polysaccharides (Dubey et al., 1998). It is likely that these complex polysaccharides are derived primarily from the carbon backbones of glycolytic intermediates. In *T. gondii*, two isoforms of the enzyme lactate dehydrogenase, which facilitates glycolytic flux by regulating pyruvate and NAD^+ levels, were found to be essential for establishing chronic infection in mice (Abdelbaset et al., 2017). In this study, we have investigated the essentiality of the *T. gondii* glycolytic enzyme hexokinase (*Tghk*) for the growth, replication and asexual differentiation of tachyzoite stage parasites. Hexokinase knockout parasites (*Δhk*; glycolytic mutant) exhibit a moderate fitness defect in vitro and decreased virulence in mice. Although *Δhk* parasites were capable of differentiating into bradyzoites in vitro, they were severely compromised in mature tissue cyst formation in vivo. Isotope-resolved metabolic labelling studies with $U^{13}C$-glucose and $U^{13}C$-$U^{15}N$-glutamine were performed to track the metabolic changes in *Δhk*, and validate glutaminolysis as the major pathway for carbon and energy acquisition in these parasites. The importance of gluconeogenesis for parasite survival in the absence of glycolysis was confirmed using *pepck1* mutant parasites (*Δpepck1*) deficient in gluconeogenesis. Further, our studies also confirm that, *T. gondii* tachyzoites are capable of maintaining cellular ATP homeostasis by via either glycolysis or mitochondrial oxidative phosphorylation.

2. Materials and methods

Detailed experimental procedures are supplied in Supplementary Data S1.

2.1. Molecular genetic methods

Parasite genomic DNA and total RNA were isolated using respective kits from Qiagen (Germany). Genomic DNA was amplified using either Herculase II Fusion (Stratagene, USA), GoTaq (Promega, USA) thermo stable DNA polymerases, or LA Taq polymerase (Takara, Japan). The *Tghk* gene knockout construct contained 1082 kb and 1126 kb flanking sequences upstream and downstream of the gene loci (TGME49_265450; ~5.3 Kb) interspaced by the canonical *T. gondii hxgprt* selection cassette (Donald et al., 1996). The *ΔhxgprtΔku80* parental strains of RH and Prugniaud *T. gondii* were transfected with a PCR amplified *Tghk* gene knockout cassette, followed by selection in the presence of mycophenolic acid and cloning stable lines of mutant parasites using the limiting dilution method. *Tghk* gene deletion was confirmed by PCR amplification of genomic DNA isolated from mutant parasites. The sequences of primers used in this study are listed in Supplementary Table S1. The *Δhk* mutants were complemented using the PSBLV72 cosmid (kindly provided from the laboratory of David Sibley, Washington University, USA), which includes the entire wild type (wt) *hk* gene loci in the middle of a ~25 kb piece of *T. gondii* chromosome IX. The constitutively expressing copy of PEPCK gene (*Tgpepck1*; TgME49_289650) was ablated via genome editing using the CRISPR/Cas9 system previously demonstrated in *T. gondii* (Shen et al., 2014; Sidik et al., 2014). The CRISPR guide RNA was engineered to target the Cas9 endonuclease to exon I of *Tgpepck1*. The Cas9 endonuclease and the guide RNA were expressed from a plasmid previously optimised for expression in *T. gondii* (Shen et al., 2014). Along with this plasmid, a PCR fragment containing the human dihydrofolate reductase (*dhfr*) gene cassette conferring pyrimethamine resistance, flanked by 40 bp of homologous region spanning the Cas9 cut site, was used to repair the Cas9 cut site resulting in targeted disruption of *Tgpepck1*. A clonal line of the *ΔTgpepck1* parasite was isolated by limiting dilution method, under pyrimethamine selection. Mutant *ΔTgpepck1* parasites were complemented with a plasmid constitutively expressing the *Tgpepck1-HA* cDNA. Clonal lines of the complemented strain were obtained by using glucose deprivation as negative selection against *Δpepck1* parasites.

2.2. Parasite strains and specific growth conditions

All experiments reported in this study were done with either RH (Type I) or Prugniaud (Pru; Type II) strains of *T. gondii*. The parasite strains used in this study are listed below and the abbreviations used to denote them are indicated within parentheses:

RH wild type (RH *wt*)
RH *ΔTghxgprtΔTgku80* (RH *Δku80*) (Fox et al., 2009; Rommereim et al., 2014)
RH *ΔTghxgprtΔTgku80ΔTghk*$^{+Tghxgprt}$ (RH *Δhk*)
RH *ΔTghxgprtΔTgku80ΔTghk*$^{+Tghxgprt+Tghk}$ (RH *Δhk*$^{+Tghk}$)
Pru *ΔTghxgprtΔTgku80* (Pru *Δku80*) (Fox et al., 2011)
Pru *ΔTghxgprtΔTgku80ΔTghk*$^{+Tghxgprt}$ (Pru *Δhk*)
RH *ΔTgpepck1* (RH *Δpepck1*)
RH *ΔTgpepck1*$^{+Tgpepck1\text{-}HA}$ (RH *Δpepck1*$^{+Tgpepck1\text{-}HA}$)

Human foreskin fibroblasts (HFF) were used as host cells for parasite infection in all experiments and routine maintenance of

tachyzoite stage parasites in the laboratory was done as previously reported (Roos et al., 1994). MEM (Invitrogen, USA) containing 5.5 mM glucose and 4 mM glutamine, in addition to salts, vitamins and essential amino acids, was used as complete medium for optimal growth of parasites. Nutrient deprivation experiments were carried out in culture medium with a similar composition but lacking either glucose or glutamine. For this, DMEM (Invitrogen) containing 4 mM glutamine and no glucose or MEM containing 5.5 mM glucose and no glutamine were used, respectively. These two media included other components such as salts, vitamins, and essential amino acids in similar proportions to those found in the complete medium, and serum was not added to any of the media used for growth assays. Two-week old confluent HFF monolayers were used for parasite growth assays, and both the host cells and parasites were washed in respective starvation mediums before setting up the infection. The viability of confluent HFF monolayers was not affected by the starvation conditions over the course of assaying parasite growth rate (typically 2–3 days) as determined by Almar Blue cell viability assays. When required, non-essential amino acids (100× MEM-NEAA; Invitrogen, USA) were added to the culture medium to a final 1× concentration. Sodium acetate, sodium pyruvate, sodium succinate dibasic hexahydrate, sodium propionate, glycerol, 2-deoxyglucose (2DG) and azaserine (all purchased from Sigma, USA) were used in specific growth experiments at concentrations given in the relevant sections.

2.3. Intracellular replication rate assays

Intracellular tachyzoites growing in complete medium were freshly released and washed in the medium of choice before being used to infect HFF monolayers in the presence of complete or minimal medium. Three to five hour p.i., the monolayers were washed with appropriate media to remove extracellular parasites. Then, parasite replication rates were determined from vacuole size as previously reported. Briefly, the vacuole size ($\log_2$ of parasite number per vacuole) was estimated for at least 100 random vacuoles in each replicate, at various times (typically with a gap of 6 or 12 h) over a period of 2–3 days depending on the strain of the parasite. The average vacuole size at each time point was used to determine the replication rate and the doubling time indicated the time taken for the parasite to divide once.

2.4. Plaque forming assays

To assess long-term growth of *T. gondii* tachyzoites under differing growth conditions, we carried out plaque forming assays. Either 200 or 50 freshly lysed tachyzoites were inoculated into a T25 culture flask or 6-well culture plates, respectively. The infected monolayers were incubated undisturbed for 8–10 days for plaque formation. To visualise the plaques, the infected monolayers where fixed with 100% ice-cold methanol and stained with crystal violet dye as previously reported (Ufermann et al., 2017). Plaque counts from each flask/well were obtained by manual inspection.

2.5. Virulence and differentiation studies in mice

Animal experiments were reviewed and approved by the Institutional Animal Care and Use Committee of Dartmouth College, Hanover, New Hampshire, USA (Animal Welfare Assurance Number #3259-01) and were performed under IACUC Protocol Number 00002108. Experiments were in accordance with the guidelines published in the Guide for the Care and Use of Laboratory Animals of the National Institutes of Health following the U.S.A. Public Health Service policy on Humane Care and Use of Laboratory Animals. Pru *Δku80* and Pru *Δhk* tachyzoites were used to assess the essentiality of glycolysis for virulence (acutely infected) and tissue cyst formation (chronically infected) in C57BL/6 mice. Acute infection was initiated by injecting mice i.p. with either a low (2×10^5) or high (2×10^6) dose of parasites. Virulence was assessed based on percent survival of mice, with daily monitoring until 100% mortality was reached in the control group of mice infected with Pru *Δku80* parasites. Chromic infection in mice was initiated by injecting ~200 tachyzoites i.p. and the cyst burden in animal brain was assessed 3 and 5 weeks p.i. as previously reported (Ferguson and Hutchison, 1987; Dubey, 1997; Bohne et al., 1998).

2.6. In vitro asexual differentiation of T. gondii and bradyzoite cyst wall staining

In vitro stage conversion studies were done essentially as previously described using the CO_2 starvation protocol (Knoll and Boothroyd, 1998). Pru *Δku80* and Pru *Δhk* tachyzoites were allowed to infect 2 week-old confluent HFF monolayers grown on glass coverslips in 6-well plates. Immediately after parasite inoculation, the plates were placed in a 37 °C incubator maintaining CO_2 at atmospheric levels (>0.04%) and at 3–5 h p.i., the infected monolayers were washed to remove extracellular parasites. The monolayers were then continuously maintained in low CO_2 condition for 1 week following which the infected monolayers were fixed and stained to visualise bradyzoite cyst wall polysaccharides. Formaldehyde (2%; Polysciences, USA) diluted in PBS was used to fix the monolayer for 10 min followed by two washes in PBS and permeablized using PBS containing Triton X-100 (Sigma). The monolayers were then blocked for 30 min in PBS containing 5% FBS and stained with 0.1 mg/ml of TRITC labelled *Dolichos biflorus* lectin (Sigma) in blocking solution. Coverslips were mounted on glass slides using Fluoromount-G (SouthernBiotech, USA) and imaged using an Olympus IX70 inverted microscope equipped with a mercury vapour lamp, appropriate barrier/emission filters (DeltaVision, USA), and a Photometrics CoolSNAP high resolution digital CCD camera.

2.7. Metabolic labelling, metabolite extraction, and LC–MS profiling

DMEM minus glucose media supplemented with $U^{13}C$-glucose (5.5 mM) and MEM minus glutamine media supplemented with $U^{13}C$-$U^{13}N$-glutamine (4 mM) were used as culture media for metabolic labelling studies using RH *wt*, RH *Δku80*, RH *Δhk*, and RH *Δpepck1* parasites. Freshly isolated extracellular (host cell-free) tachyzoite stage parasites were washed once in complete medium and resuspended in either ^{13}C labelled glucose or glutamine (Cambridge Isotope Laboratories, Inc., USA) containing medium at a density of 10^8 parasites per millilitre. Labelling was allowed to proceed over a time period of 5, 10, 15, 30, 60 and 120 min in 1 ml of culture suspension. At each time point, metabolites were extracted from replicate parasite samples using a modified version of a previously reported protocol (Olszewski et al., 2009). Briefly, host cell-free parasites were collected by centrifugation at 1650*g* for 5 min at 4 °C, the supernatant was removed, and the cell pellet immediately resuspended in 200 µl of ice cold 80% acetonitrile (Chem-Impex; JT Bakers, USA) in water and incubated on ice for 15 min with intermittent vortexing. The supernatant was then collected after centrifuging at 16,200*g* for 5 min and the pellet was further extracted twice with 100 µl of the same solvent using ultrasound in a sonicating iced water bath for 15 min. All the extracts were pooled (total 400 µl) and stored in −80 °C until further processing for LC–MS analysis.

The acetonitrile:water extracts from parasites were dried under nitrogen flow and resuspended in 200 µl of water:methanol (97:3) containing 10 mM tributylamine and 15 mM acetic acid. This solvent was also used as buffer A and methanol as buffer B for liquid chromatography using a Synergy Hydro-RP column (Phenomenex,

USA) with a bed volume of 100 mm × 2 mm and particle size of 2.5 μ. For some samples, an alternate method was used, with an Accucore C18 column (Thermo Fisher Scientific, USA) with a bed volume of 150 mm × 2.1 mm and 2.6 μ particle size. A solvent system composed of water buffered with 0.1% formic acid (buffer A) and acetonitrile (buffer B), was used on a 20 min gradient run with a flow rate of 200 μl/min as follows: hold at 10% acetonitrile for 30 s and gradually ramp up to 15%, 20%, 50%, 60% and 90% acetonitrile by 3, 6, 10, 12, 13 min, hold at 90% acetonitrile until 15 min, ramp down to 10% acetonitrile by 15.5 min and hold until 20 min. LC–MS analysis was done using a Exactive Orbitrap mass spectrometer, coupled to an Accela U-HPLC (Thermo Fisher Scientific) and HTC PAL autosampler (CTC Analytics AG, Switzerland). The mass spectrometer was run in negative mode, scanning a mass-charge ratio (*m/z*) range of 85–1000. All other parameters used for LC–MS instrumentation in this study were similar to published protocols (Lu et al., 2010; Melamud et al., 2010).

2.8. LC–MS data processing and analysis

The RAW file output from the mass spectrometer was converted from the profile mode into centroid mode using the ReAdW or Proteowizard programme (Chambers et al., 2012) and further analysed using the MAVEN (Clasquin et al., 2012) programme. Data from replicate samples for each time point was aligned within MAVEN and ion chromatograms were extracted for each compound to within a 10 PPM window of the expected *m/z* value. Peaks were detected from these ion chromatograms and their quality was ascertained using default settings available in MAVEN. Metabolites were identified by matching the retention times as well as the *m/z* values to >99% pure commercial standards for which in-house calibration was done. Grouped peaks from replicate samples for all time points were matched to the expected retention time of standards, and the peaks with a quality score of at least 0.5 were hand picked for metabolites of interest. In addition to the $^{12}C/^{14}N$ containing parent compounds, $^{13}C/^{15}N$ labelled isotopomers for each metabolite were selected by accounting for the expected shift in *m/z* values. Peak height was used as a measure of metabolite abundance and in case of ^{13}C labelled compounds, we also accounted for the natural distribution of the isotope as calculated by the Qual Browser included in the Xcalibur software suite (Thermo Fisher Scientific) and corrected the final signal output accordingly. The relative abundance of unlabelled and ^{13}C labelled isotopomers of each metabolite was calculated for all samples over the experimental time course. Signals obtained from blank runs were used for noise correction and only peaks with a signal intensity of at least 1000 counts (approximate instrument limit for quantitation) were considered. Since we expected the signal levels of metabolites to change across the experimental time points (especially for isotopically labelled forms), we considered metabolites that had a signal count of 1000 or more in at least one time point. The ^{13}C labelled isotopomers of metabolites were plotted only if they represented 10% or more of the total metabolite pool in at least one time point. Although we could reliably detect between 50 and 100 different metabolic intermediates from the different samples (in addition to hundreds of other unknown mass features), only a few key intermediates of glycolysis, pentose phosphate pathway and the Krebs cycle are presented, as these are relevant to the studies performed here. The raw and processed data from metabolomics studies has been deposited in the metabolomics workbench repository under the study ID ST000817.

2.9. Measuring total cellular ATP content in T. gondii

ATP was measured in extracellular tachyzoite stage parasites suspended in complete media or media lacking glucose or glutamine. Freshly isolated tachyzoites from infected monolayers were separated from host cell debris, collected by centrifugation (1650*g* for 5 min at 25 °C) and washed once in the medium of choice before being resuspended in the same medium at a density of 2×10^6 parasites/ml. The suspension (10^5 parasites in 50 μl) was added to individual wells in a white opaque 96-well plate pre-seeded with 50 μl of appropriate culture medium. In experiments using atovaquone, the pre-seeded medium contained 2, 20 or 200 nM of the drug or 1% DMSO only as control. To assess the effect of nutrient deprivation on ATP synthesis, a time course experiment was carried out in which parasites incubated in different media were sampled for total cellular ATP content at 0.5, 1, 2, 3, 9 and 15 h. For assessment of the effect of atovaquone on ATP synthesis in conjugation with nutrient starvation, ATP content was measured in parasites at a fixed time point of 2 h after exposure to atovaquone. ATP content in *T. gondii* was measured using the firefly luciferase activity-based ATPlite assay kit (Perkin Elmer, USA). The luciferase activity is directly proportional to the free ATP available from the parasite cell to drive the light emitting reaction. The luminescence readouts where measured using the Analyst HT system (LjL Biosystems, USA) and accompanying CriterionHost software (Molecular Devices, USA).

3. Results

3.1. Glucose and glycolytic enzyme hexokinase are not essential for T. gondii tachyzoites

In agreement with previous reports (Blume et al., 2009; Nitzsche et al., 2016), we found that *T. gondii* tachyzoites were capable of continuously propagating in the absence of glucose in culture medium. Glucose-deprived tachyzoite stage parasites exhibit only a moderate fitness defect (doubling time ~9 h) in comparison with growth in the presence of 5.5 mM glucose (doubling time ~7 h) (Supplementary Fig. S1A). Glutamine (4 mM) alone as a carbon source was sufficient to support parasite growth in the absence of glucose, and the addition of other carbon sources such as pyruvate, acetate, succinate, glycerol and propionate (5 mM each) did not help in restoring optimal growth of the parasite. Continuous culturing of tachyzoite stage parasites in the absence of glucose did not result in progressive loss or gain of parasite fitness. In fact, glucose-deprived parasites were capable of immediately resuming optimal growth, without any lag, when again provided with glucose (Supplementary Fig. S1B). These observations highlight the ability of tachyzoite stage *T. gondii* to adapt their growth in response to nutrient availability. We also noted that nutrient stress imposed by continuous cultivation of *T. gondii* tachyzoites in the absence of glucose did not lead to asexual stage conversion or induction of bradyzoite-specific markers (data not shown).

Since *T. gondii* tachyzoites are capable of scavenging a variety of metabolites from host cells, it is likely that when deprived of external glucose, they can acquire host-derived glucose. This was observed in the earlier work, where residual glycolytic activity is detectable in *Δgt1* mutants parasites (Nitzsche et al., 2016). To further validate the essentiality of glucose and its metabolism via glycolysis in *T. gondii*, we proceeded to knock out the single copy *hk* gene (*Tghk*; TGME49_265450), which catalyses the first step in glycolysis. In the absence of hexokinase, the parasites cannot metabolise glucose even if it is available. We generated *Tghk* gene knockout parasites in both RH and Pru strains of *T. gondii* (from the respective *Δku80* parental strains) via homologous recombination mediated gene replacement, in which part of the *Tghk* gene locus was replaced by the *Tghxgprt* selection cassette. The absence of the *Tghk* gene was confirmed by genomic PCRs (in RH and Pru strains; data not shown) and by DNA microarray analysis (in RH only) using the Affymetrix Toxoarray (Bahl et al., 2010)

(Supplementary Fig. S2A). Obtaining *Δhk* mutants in two different strains of *T. gondii* further confirmed that glucose and glycolysis are not essential for survival of tachyzoite stage parasites.

3.2. Pharmacological validation of δtghk parasites using 2DG as a metabolic probe

Toxoplasma gondii encodes all enzymes necessary for reverse synthesis of glycolytic intermediates via gluconeogenesis (ToxoDB.org) and this pathway is important for metabolic adaptation during glucose deprivation (in RH *wt*) or when the parasites are not capable of oxidising glucose (in RH *Δhk*). In fact, there was no detectable difference in replication rate kinetics of RH *Δhk* parasites in the presence (doubling time ~8.9 h) or absence (doubling time ~9.1 h) of glucose (Fig. 1A). For functional validation of *hk* gene knockout, we used 2DG as a metabolic probe. 2DG is a structural analogue of glucose that can be transported into cells via the glucose transporter and is converted by hk into 2-deoxyglucose-6-phosphate (2DG-6P), an anti-metabolite which inhibits glucose-6-phosphate dependent enzymes (Barban, 1962). The EC_{50} for 2DG-mediated parasite killing was ~500 μM. Treatment with 5 mM 2DG completely inhibited RH *wt* parasite growth resulting in their death, but only in the absence of glucose (Fig. 1B, Supplementary Fig. S3A). Glucose (1 mM) was capable of completely reversing the growth inhibitory effects of 2 mM 2DG (Supplementary Fig. S3B). These results are consistent with the fact that glucose is the preferred substrate over 2DG, for the hk enzyme.

In contrast, the growth of RH *Δhk* parasites (doubling time ~9.1 h) was not affected by 5 mM 2DG, even in the absence of glucose (Fig. 1A), thus functionally validating the *hk* knockout. However, RH *Δhk* parasites complemented with a functional *hk* gene (RH Δhk^{+Tghk}) were susceptible to growth inhibition by 5 mM 2DG in the absence of glucose (Supplementary Fig. S4A). It should also be noted here that any 2DG-6P produced inside the host cell (by host hk activity) is not inhibitory to parasite growth. This supports the notion that phosphorylated metabolites such as intermediates of glycolysis are not available from the host cells at sufficient concentrations for uptake by the parasite.

3.3. In vivo virulence and differentiation studies with Δhk parasites

Since glucose is physiologically the most abundant nutrient in the host, it is readily available for the parasite. In studies with *Δgt1* parasites, it was found that the in vivo virulence of the mutant parasite is not compromised (Blume et al., 2009). In accordance with this, we found that the parasite burden achieved following acute intra-peritoneal infection of mice with 200 RH *Δhk* tachyzoites was comparable with that seen with RH *wt* parasites (data not shown). However, since our interest was to study the importance of glycolysis for asexual differentiation in vivo, further experiments were conducted with Pru *Δhk* parasites. We first monitored virulence following acute infection with either the parental Pru or mutant Pru *Δhk* tachyzoites, each in two different doses of 2×10^5 (low) and 2×10^6 (high) parasites. In the low dose group (Fig. 2A), three out of four mice infected with parental Pru parasites succumbed to infection before day 10, while the 4th mouse died at day 40. However, none of the mice infected with low dose of Pru *Δhk* parasites succumbed to infection until day 40. In the high dose group, all mice infected with either the *wt* or *Δhk* parasites strains died before day 10 (Fig. 2A).

In contrast to the outcome of acute infection, during chronic infection mice infected with 200 Pru *Δhk* parasites showed a drastically reduced cyst burden (by ~97%) (Fig. 2B) when compared with mice infected with parental wt parasites. In order to determine whether the inability of Pru *Δhk* parasites to form productive tissue cysts in vivo was due to defective cyst wall formation, we checked to see if these parasites are capable of in vitro

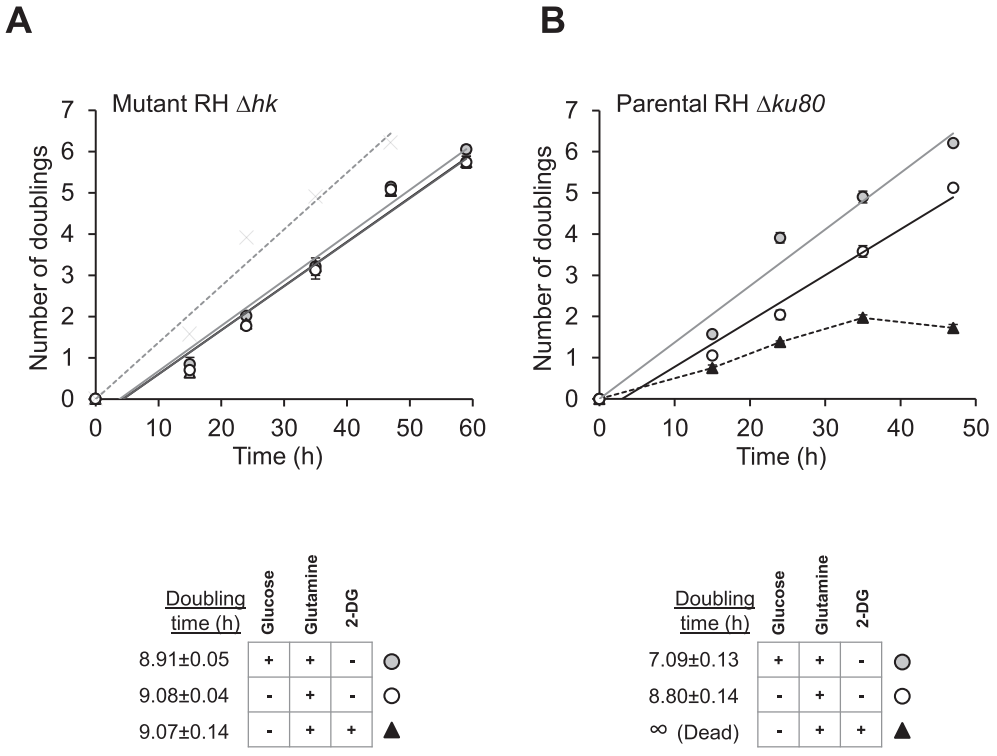

Fig. 1. Replication studies with *Toxoplasma gondii* RH *Δhk* and RH *Δku80* parasites. Replication kinetics of RH *Δhk* (A) and RH *Δku80* (B) tachyzoite stage parasites in the presence and absence of glucose and 2-deoxyglucose. The grey dashed line in (A) indicates the replication rate of parental strain in optimal growth conditions. The dashed line in (B) indicates that parasites stop replicating and die when treated with 2-deoxyglucose concomitant with glucose deprivation. *hk*, hexokinase.

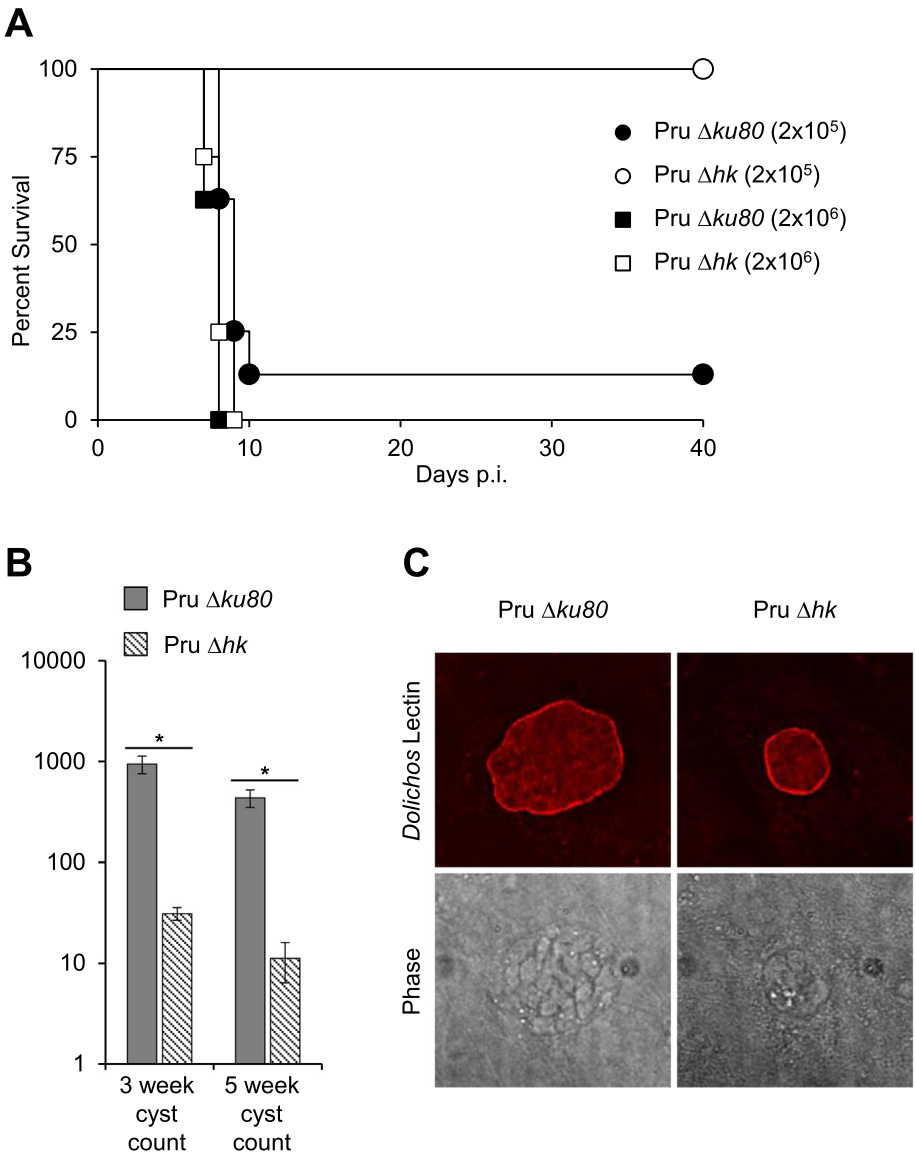

Fig. 2. Acute virulence in mice and asexual differentiation of Pru *Δku80* and Pru *Δhk* strains of *Toxoplasma gondii*: (A) Survival curves for mice following i.p. injection with either 2×10^5 or 2×10^6 tachyzoites of *T. gondii* RH *Δku80* or RH *Δhk* parasites, respectively. (B) Estimation of cyst burden in mouse brain following establishment of chronic infection with Pru *Δku80* and Pru *Δhk* parasites. $^*P = 0.0001$. (C) *Dolichos biflorus* lectin staining was done to visualise the presence of cyst wall polysaccharide during in vitro asexual differentiation of Pru *Δku80* and Pru *Δhk* parasites. The vacuole formed by the Pru *Δhk* parasite is smaller owing to the decreased fitness of the mutant parasite. Staining was done after 1 week of growth under optimal conditions required for inducing bradyzoite differentiation in vitro. *hk*, hexokinase.

differentiation and cyst wall formation. Pru *wt* and Pru *Δhk* infected host cells were maintained under low CO_2 conditions for 1 week and then stained for cyst wall formation using *Dolichos biflorus* lectin (Boothroyd et al., 1997). We observed that the Pru *Δhk* parasites were equally competent as Pru *wt* parasites in initiating bradyzoite differentiation and forming the cyst wall in vitro (Fig. 2C). Therefore, it appears that glutamine metabolism can support cyst wall biogenesis and other metabolic requirements associated with early bradyzoite differentiation. However, deficient mature tissue cyst formation in vivo might indicate that glucose metabolism is essential for this process. In addition, glycolysis is probably essential for dissemination of tachyzoites to favourable tissue locations for productive tissue cyst formation and persistence in the host.

3.4. Metabolic impact of deficient glucose metabolism

To study the metabolic changes in *Δhk* parasites, we carried out metabolic labelling studies with extracellular tachyzoites. Following isotopic labelling, total metabolites were extracted from parasites and profiled by LC–MS. The kinetics of ^{13}C assimilation from $U^{13}C$-glucose and $U^{13}C$-$U^{15}N$-glutamine was tracked over a period of 2 h. Our primary focus was to analyse metabolic intermediates from glycolysis, the pentose phosphate pathway and the Krebs cycle as these pathways are directly impacted by glucose or glutamine availability and are the key pathways via which bulk assimilation of carbon likely occurs in *T. gondii* (MacRae et al., 2012; Oppenheim et al., 2014).

When RH *wt* parasites were fed $U^{13}C$-glucose (in the presence of unlabelled glutamine), robust labelling was observed for intermediates of glycolysis and the pentose phosphate pathway, together with minimal labelling in Krebs cycle intermediates (Fig. 3A). We noticed that $+2^{13}C$-acetyl-CoA derived from glucose was incorporated into citrate, as previously reported (Oppenheim et al., 2014). On the other hand, when parasites were fed with $U^{13}C$-$U^{15}N$-glutamine (in the presence of unlabelled glucose), labelling was restricted to intermediates of the Krebs cycle only

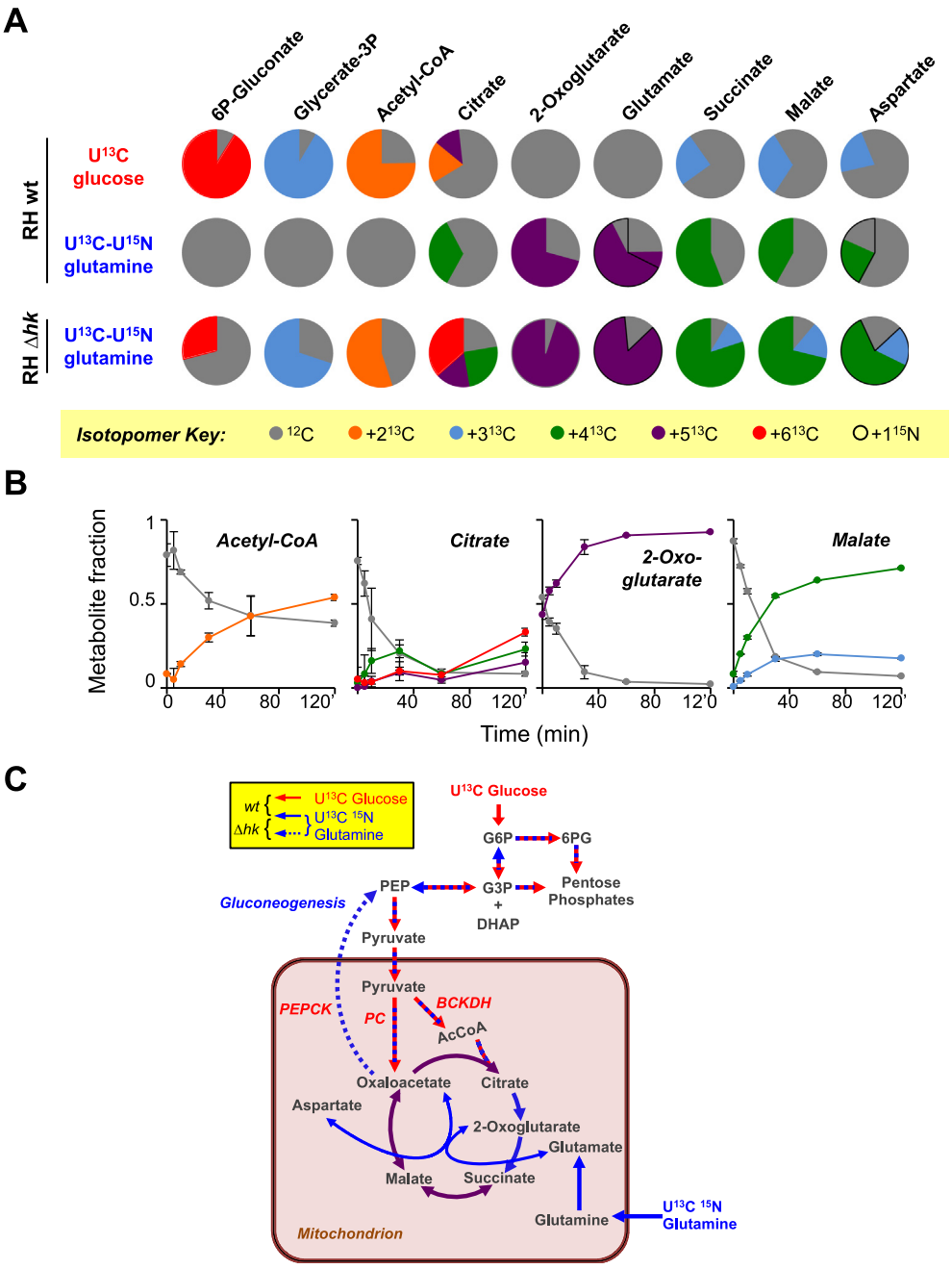

Fig. 3. Metabolite profiling in *Toxoplasma gondii* RH *wt* and RH *Δhk* parasites. U^{13}C-glucose and U^{13}C-U^{15}N-glutamine were used as metabolic tracers to track the flux of ^{13}C carbon derived from these nutrients. (A) Pie charts indicate the fraction of ^{13}C labelled isotopomers in the total metabolite pool for key intermediates from pentose phosphate pathway, glycolysis and Krebs cycle after 120 min of labelling. For labelling kinetics for these metabolites, see Supplementary Figs. S5, S6. The colour key indicates the different isotopomers. (B) Kinetic profile of ^{13}C-isotopomer formation for acety-CoA, citrate, 2-oxoglutarate and malate following labelling of RH *Δhk* parasites labelled with U^{13}C-U^{15}N-glutamine. The colour scheme is same as in (A). (C) Summary of the ^{13}C flux in intermediates of glycolysis, pentose phosphate pathway and Krebs cycle in RH *wt* and RH *Δhk* parasites. Arrow colours indicate: red, labelling seen with glucose (in RH *wt* only); purple, labelling seen with glucose (in RH *wt* only) and glutamine (in RH *wt* and RH *Δhk*); solid blue, labelling seen with glutamine (in RH *wt* and RH *Δhk*); dotted blue, labelling seen with glutamine (in Rh *Δhk* only). Data shown is from three replicates. *hk*, hexokinase; *wt*, wild type.

and no labelling was detected in any intermediates of glycolysis or the pentose phosphate pathway. This confirms that gluconeogenesis is inactive when glycolysis is active, as observed previously (Oppenheim et al., 2014). Notably, acetyl-CoA remained unlabelled and there was no evidence for acetyl-CoA derived labelling of citrate. It is evident from these labelling patterns that glucose and glutamine have distinct metabolic fates in wild type *T. gondii* tachyzoites (Fig. 3A). In contrast to *wt* parasites, U^{13}C-glucose derived labelling was completely absent in *Δhk* parasites (Supplementary Fig. S5), further confirming the inability of these parasites to metabolise glucose.

However, RH *Δhk* parasites readily incorporated ^{13}C- derived from U^{13}C-U^{15}N-glutamine into intermediates of the Krebs cycle. Importantly, unlike in *wt*, ^{13}C label was not restricted to the Krebs cycle, and significant levels of ^{13}C incorporation was also observed in intermediates of glycolysis and the pentose phosphate pathway

(Fig. 3A). Thus, in *Δhk* parasites gluconeogenesis is required for maintenance of glycolytic and pentose phosphate pathway intermediates.

3.5. Insights into the central carbon metabolism of T. gondii

The kinetics of ^{13}C-labelling for intermediates of glycolysis and Krebs cycle revealed the dynamics of carbon flux between these pathways. U^{13}C-pyruvate derived from glycolysis is converted in the mitochondrion to +2^{13}C-acetyl-CoA, by BCKDH (Oppenheim et al., 2014), and +3^{13}C-oxaloacetate, by pyruvate carboxylase enzyme (MacRae et al., 2012). Although we do not detect oxaloacetate in our LC–MS method, we can infer its labelling pattern from the +3^{13}C- isotopomers detected for aspartate (formed by transamination of oxaloacetate), citrate and malate (Supplementary Fig. S5). We detected +2^{13}C and +5^{13}C isotopomers for citrate, indicating that +2^{13}C-acetyl-CoA was combining with both unlabelled and +3^{13}C-oxaloacetate to form citrate. Interestingly, we did not see any exchange of ^{13}C- between citrate and 2-oxoglutarate, and much of citrate remained unlabelled by glucose.

The labelling patterns observed with U^{13}C-glucose were well complemented by U^{13}C-U^{15}N-glutamine labelling patterns. First, U^{13}C-U^{15}N-glutamine is deaminated to U^{13}C-+1^{15}N-glutamate, which is then transaminated to form U^{13}C-2-oxoglutarate. Following this, +4^{13}C- isotopomers of succinate, fumarate, malate, oxaloacetate and citrate are formed. Unlabelled and +4^{13}C-oxaloactetate participate in the transamination of glutamate to aspartate, resulting in the formation of +1^{15}N- and U^{13}C-+1^{15}N-aspartate (Supplementary Fig. S5). The lack of glutamine-derived ^{13}C-labelling in glycolytic intermediates and acetyl-CoA indicates that steady state glycolytic flux prevents gluconeogenesis. Here again, as in case of U^{13}C-glucose labelling, we did not observe any flux of ^{13}C- from citrate to 2-oxoglutarate. If +4^{13}C-citrate were to be converted to 2-oxoglutarate, since one of the carbon atoms derived from oxaloacetate is lost as CO_2, +3^{13}C-2-oxoglutarate should be formed. However, only U^{13}C-2-oxoglutarate obtained from transamination of glutamate was detected, suggesting that citrate may not cycle back into the Krebs cycle. Possibly citrate might act as a carbon sink in the mitochondrion, which can be shuttled out into the cytosol and be split into acety-CoA and oxaloacetate by the cytosolic ATP-citrate lyase enzyme (Oppenheim et al., 2014; Tymoshenko et al., 2015; Nitzsche et al., 2016). Cytosolic oxaloacetate can be recycled to the mitochondrion via the citrate-malate shuttle, where oxaloacetate is first converted into malate, by cytosolic malate dehydrogenase (ToxoDB gene ID TGME49_318430), which is then imported into the mitochondrion via the 2-oxoglutarate/malate translocase (ToxoDB gene ID TGME49_274060).

When *Δhk* parasites were fed U^{13}C-U^{15}N-glutamine, the isotopomer profile of Krebs cycle intermediates resembled a combination of the profile obtained for glucose or glutamine labelling in *wt* parasites (Fig. 3B, Supplementary Fig. S5). However, unlike in *wt*, we observed the formation of +3^{13}C-glycerate-3-phosphate and U^{13}C-6-phospho gluconate, suggesting that gluconeogenesis is functional in *Δhk* parasites. In addition to forming glycerate-3-phosphate (gluconeogenesis), phosphoenolpyruvate (PEP) also facilitates the production of pyruvate, which is then converted to acetyl-CoA and oxaloacetate in the mitochondrion. This is supported by the formation of +2^{13}C-acetyl-CoA and +3^{13}C- isotopomers for malate, succinate and aspartate in *Δhk* parasites, in the presence of U^{13}C-U^{15}N-glutamine. In *wt* parasites, a similar isotopomer profile for these metabolites is seen only in the presence of U^{13}C-glucose. Moreover, the formation of +4^{13}C-, +5^{13}C- and U^{13}C- isotopomers of citrate suggests that +3^{13}C- and +4^{13}C- isotopomers of oxaloacetate and +2^{13}C-acetyl-CoA contribute to citrate formation (Supplementary Fig. S5). As in *wt* parasites, in *Δhk* parasites also there was no evidence for the cyclic operation of Krebs cycle, as shown by the completed absence of +3^{13}C- isotopomer for 2-oxoglutarate. A summary of the metabolic circuitry in both *wt* and *Δhk* parasites, based on the observed ^{13}C- isotopmer profiles is shown in Fig. 3C and elaborated in Supplementary Fig. S6.

3.6. Importance of glutamine in Δhk parasites

Replication, differentiation, and metabolic profiling studies with *wt* and *Δhk* parasites revealed that glutamine is a key nutrient for the parasite. We therefore tested glutamine essentiality in *wt* and *Δhk* parasites. When *wt* tachyzoites were deprived of external glutamine (in the presence of glucose), they showed a slight, but consistent, fitness defect (doubling time ~8.8 h) (Fig. 4A). The fact that we see a fitness defect in the absence of glutamine, even when glucose is available, suggests a distinct metabolic role for glutamine. This fitness defect was reversed by the addition of a cocktail of non-essential amino acids containing aspartate, alanine and glutamate, but lacking glutamine. Surprisingly, *Δhk* parasites remained viable in the absence of glutamine, and exhibited a fitness defect (over that already imposed by lack of glycolysis; doubling time ~12.6 h), which was reversed by the addition of a cocktail of non-essential amino acids (Fig. 4B). *Δhk* parasites probably survive in the absence of external glutamine by scavenging glutamine from the host cells. We tested this possibility by using the glutamine analogue azaserine, which is an inhibitor of glutamine synthetase (Lea and Miflin, 1975; Rowell et al., 1977). In the absence of exogenous glutamine, 10 μM azaserine completely inhibited *wt* parasite growth and resulted in their death; NEAAs did not rescue parasites from azaserine mediated death (Supplementary Fig. S7), suggesting that glutamine is essential for parasite survival.

While performing glutamine deprivation experiments with *Δhk* parasites, we noticed a dramatic reduction in the number of parasite vacuoles per microscopic field. We investigated this observation further by performing plaque assays, and found that the plaquing efficiency of *Δhk* tachyzoites was reduced by >95% in the absence of glutamine, suggesting a dramatic reduction in invasion efficiency in comparison with *wt* parasites (Fig. 4C). However, unlike intracellular growth, the invasion defect of extracellular *Δhk* parasites was not reversed by non-essential amino acids. It is likely that ATP synthesis is compromised in extracellular *Δhk* parasites in the absence of glutamine, as was previously reported in case of *wt* and *Δgt1* parasites (MacRae et al., 2012; Nitzsche et al., 2016).

3.7. Conditional essentiality of PEPCK in T. gondii

It is apparent from our metabolic labelling studies that the PEPCK enzyme is critical for gluconeogenesis, and is likely essential for parasite growth in the absence of glycolysis. The role of PEPCK and its essentiality in *Δgt1* parasites was previously reported (Nitzsche et al., 2017). To further validate these findings and study ATP biogenesis in parasites deficient in gluconeogenesis, we generated mutant parasites lacking a functional PEPCK enzyme. Two isoforms of PEPCK are encoded by *T. gondii*, TgME49_289650 (*Tgpepck1*) and TgME49_289930 (*Tgpepck2*), of which only the former is expressed and likely functional in tachyzoites (*Toxodb.org*). Using the CRISPR/Cas9 mediated genome editing approach, we obtained *Tgpepck1* gene knockout (*ΔTgpepck1*) parasites in the RH strain of *T. gondii* (Fig. 5A). The mutant genotype was confirmed by genomic PCRs, and lack of *Tgpepck1* mRNA expression was confirmed by cDNA PCRs (Fig. 5B).

Replication assays with *Δpepck1* parasites revealed a marginal fitness defect under optimal growth conditions (doubling time ~9.5 h). While glutamine was not essential for RH *Δpepck1*

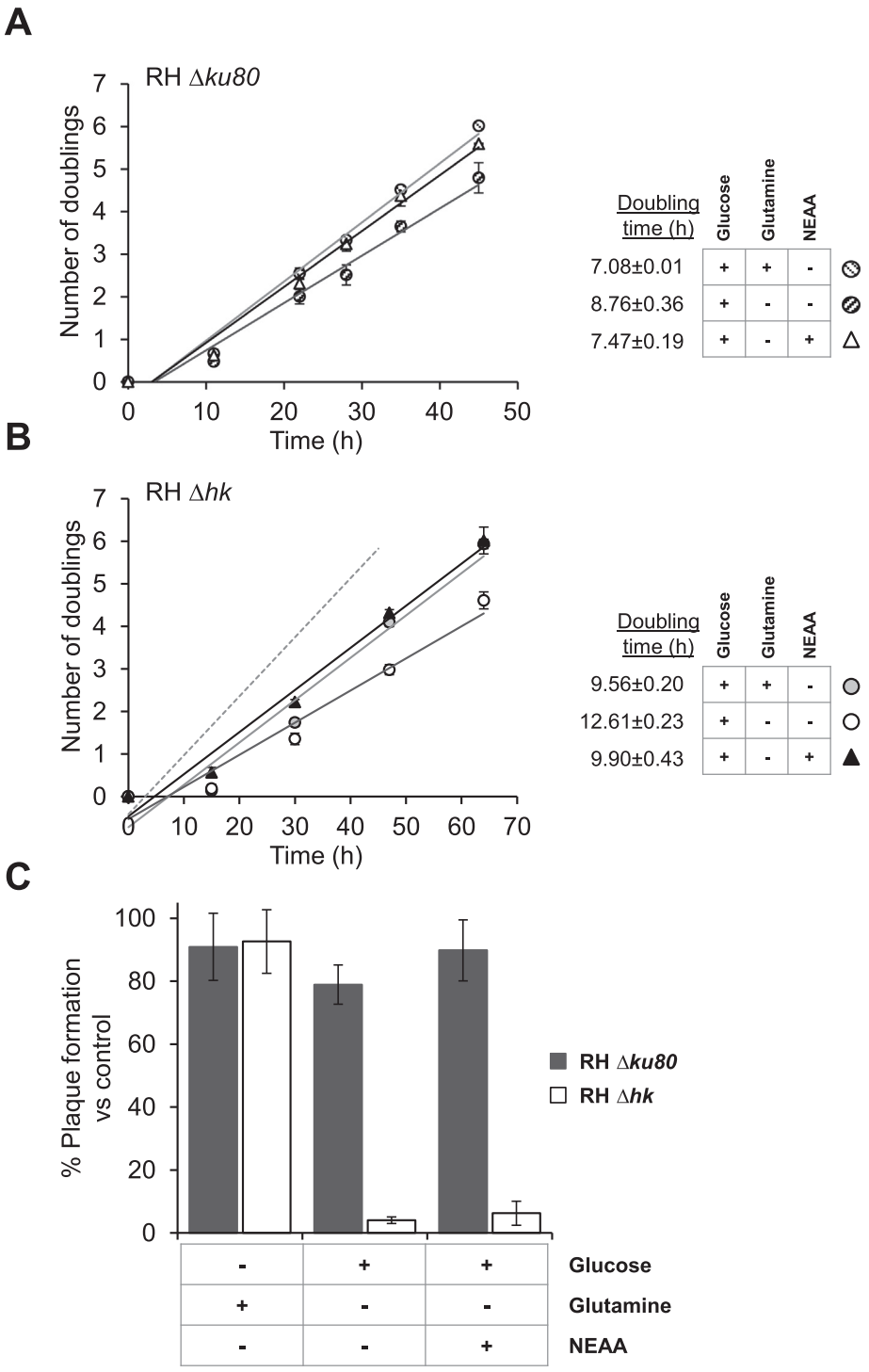

Fig. 4. Replication kinetics and plaque formation assays following glutamine deprivation. Replication assays for *Toxoplasma gondii* tachyzoite stage RH *wt* (A) and RH *Δhk* (B) parasites in the presence and absence of glutamine and non-essential amino acids (NEAA). The grey dashed line in (B) indicates the growth of RH Δ*ku80* parental strain under optimal conditions. (C) Plaque formation assays were carried out to determine the ability of the parasites to invade and replicate within host cells in the absence of glutamine. The number of plaques formed was normalised to control cultures of respective parasites growing in complete media. *hk*, hexokinase; *wt*, wild type.

parasite growth (doubling time ~9.4 h), glucose deprivation was found to be lethal for these parasites (Fig. 5C). We performed plaque assays to demonstrate that the *Δpepck1* parasites were actually dead and not merely growth arrested when deprived of glucose. For this, the *Δpepck1* parasites were first grown in the absence of glucose for 24, 48 or 72 h, before again adding glucose to the culture and allowing the parasites to form plaques. We found that *Δpepck1* parasites can survive glucose deprivation for up to 48 h, albeit with decreased plaque-forming efficiency. However, after 72 h of glucose deprivation, no plaque formation was observed, suggesting that the parasites cannot survive glucose deprivation beyond 48 h (Supplementary Fig. S8). Moreover, acetate supplementation did not reverse the replication defect observed with *Δpepck1* parasites in the absence of glucose (Supplementary Fig. S9). Metabolic labelling studies on *Δpepck1* parasites using $U^{13}C$-$U^{15}N$-glutamine revealed the absence of

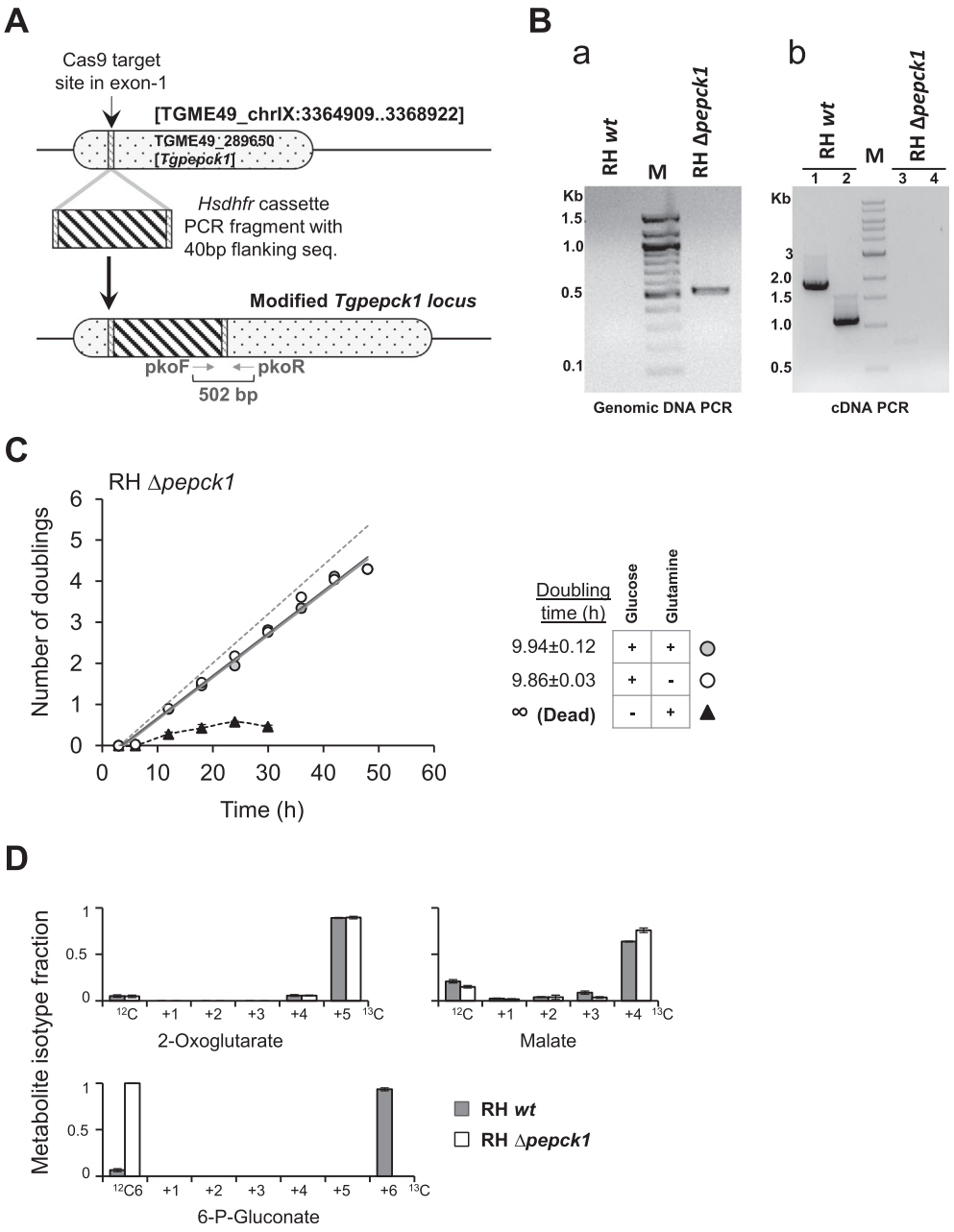

Fig. 5. *Toxoplasma gondii* phosphoenolpyruvate carboxykinase (*Tgpepck1*) gene knockout studies. (A) Schema depicts the strategy used for knocking out *Tgpepck1* gene using the CRISPR/Cas9 system; the CRISPR guide RNA was designed to target exon-1 of the gene. (B) Confirmation of *Tgpepck1* gene knockout by (Ba) genomic DNA and (Bb) cDNA PCRs. (Ba) A 502 bp PCR product is amplified from genomic DNA of RH *Δpepck1* parasites only, using the primer pairs pkoF and pkoR shown in (A). M, 100 bp DNA marker ladder. (Bb) In cDNA PCRs, exon-specific primers were used to amplify two different PCR products, 1835 bp fragment (lane 1) and 1079 bp fragment (lane 2). M, 1 kb DNA marker ladder. (C) Replication assay for RH *Δpepck1* tachyzoites in the presence and absence of glucose or glutamine. The black dashed line indicates that RH *Δpepck1* parasites are killed by glucose deprivation. The grey dashed line indicates the growth of RH *wt* parasites in complete media. (D) ^{13}C labelling pattern derived from U^{13}C-U^{15}N-glutamine in the absence of glucose for intermediates of Kreb's cycle (2-oxoglutarate and malate) and pentose phosphate pathway (6-P-gluconate) from RH *wt* and RH *Δpepck1* parasites. Lack of +6^{13}C labelling for 6-P-gluconate demonstrates the absence of gluconeogenesis in RH *Δpepck1* parasites. ^{13}C labelling data shown is from three replicates. *wt,* wild type; *Hsdhfr*, human dihydrofolate reductase.

gluconeogenic flux of ^{13}C- from Krebs cycle to glycolytic and pentose phosphate pathway intermediates (Fig. 5D). These findings are in agreement with that previously reported using conditional expression of *Tgpepck1* in *Δgt1* parasites (Nitzsche et al., 2017).

While performing complementation studies with *Δpepck1* parasites, we tested the possibility of using glucose deprivation as selection for transgenic parasites expressing *Tgpepck1*. *Δpepck1* tachyzoites, transfected with a *T. gondii* expression plasmid encoding the *Tgpepck1* cDNA with an in-frame haemagglutinin (HA) tag at the 3′ end (*Tgpepck1-HA*), were allowed to replicate in minus glucose medium. The surviving parasites were found to be 100% positive for *Tg*PEPCK-HA expression, and the localization was cytosolic as confirmed by immunostaining with anti-HA antibodies (Supplementary Fig. S10A). *Tgpepck1* has a mitochondria localization signal (as predicted by *TargetP 1.1*), and upon addition of a HA tag in the 3′ end of the gene in the genomic locus and expression from the native promoter confirmed that PEPCK1-HA localised to the mitochondria (Nitzsche et al., 2017). In our study, it appears that the overexpression of the *Tgpepck1-HA* cDNA from a plasmid using the β-tubulin promoter has resulted in mis-localization to

the cytosol. Nevertheless, the cytosol localised PEPCK1-HA protein functionally complemented the mutant phenotype. Replication assays carried out on complemented parasites (RH *Δpepck1*$^{+Tgpepck1\text{-}HA}$) had comparable growth to *wt* parasites in the absence of glucose (Supplementary Fig. S10B).

3.8. Glutaminolysis facilitates mitochondrial oxidative phosphorylation

The F-type ATP synthase in apicomplexan mitochondrion is highly divergent (Gardner et al., 2002; Mather et al., 2007; Brayton et al., 2007; Reid et al., 2012) and many of its subunits are not readily detected by sequence comparison with yeast and mammalian counterparts. However, evidence is now available for the existence of a functional F-type ATP synthase in *T. gondii* mitochondrion (Lin et al., 2011). We reasoned that in the absence of glycolytic ATP, RH *Δhk* parasites should be wholly dependent on mitochondrial ATP. This assumption is supported by our observation that extracellular *Δhk* parasites deprived of glutamine are unable to invade host cells efficiently. In order to validate this, we tracked ATP synthesis in extracellular tachyzoites incubated in the presence and absence of glucose for 15 h (Fig. 6A). In *wt* parasites, ATP levels decreased to ~50% in 6 h, coinciding with the half-life of extracellular parasite viability (Konrad et al., 2011). Importantly, the kinetics of ATP loss in *wt* was similar in complete, minus glucose and minus glutamine medium, suggesting that either glucose or glutamine alone as a nutrient can sustain optimal cellular ATP levels. In *Δhk* parasites, presence/absence of glucose had no effect on ATP homeostasis and the kinetics of ATP loss was similar to that of *wt*. However, when *Δhk* parasites were deprived of glutamine, ATP levels declined dramatically; ~50% loss was seen in less than 2 h, and by ~6 h there was complete loss of ATP (Fig. 6B). Non-essential amino acids could not rescue the ATP synthesis deficiency in *Δhk* parasites.

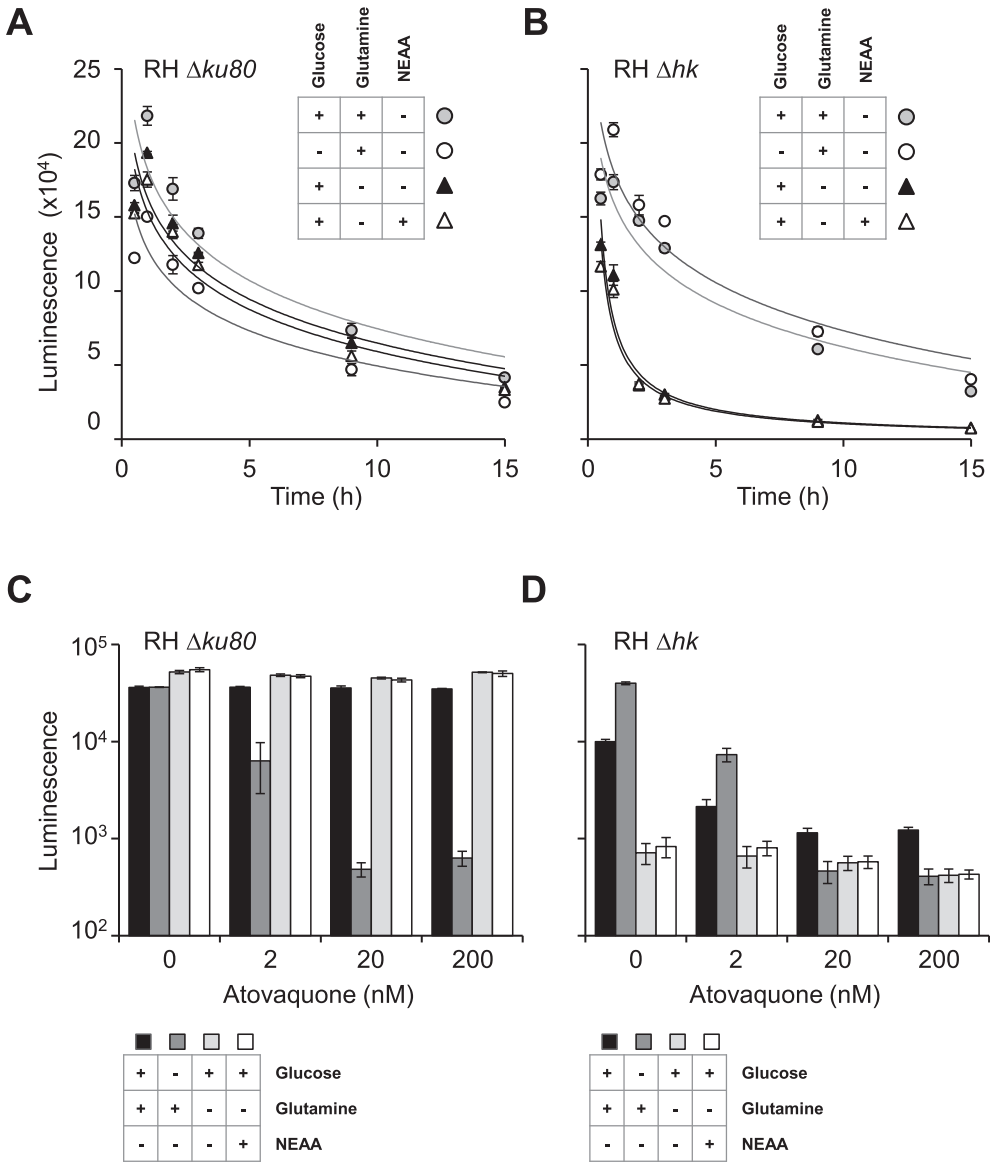

Fig. 6. ATP synthesis assays on tachyzoite stage *Toxoplasma gondii*. Luciferase expressing, extracellular parasites were used to measure total cellular ATP content. Progressive loss of ATP with time can be seen in Rh *wt* (A) and RH *Δhk* (B) parasites incubated in complete and nutrient-deficient media. Since RH *Δhk* parasites are always dependent on glutaminolysis for ATP synthesis, when deprived of glutamine, they exhibit a dramatic loss of cellular ATP, with a half-life of ~1–2 h. (C, D) Effect of atovaquone on ATP synthesis in RH *wt* and RH *Δhk* parasites, following 2 h of drug treatment. Here again, the parasites were incubated in complete and nutrient-deficient media. Three replicate samples were used in all assays. NEAA, mixture of non-essential amino acids; *wt*, wild type, *hk*, hexokinase.

We validated these findings using atovaquone, which inhibits oxidative phosphorylation (McFadden et al., 2000). Atovaquone targets the CYTb protein of the mitochondrial electron transport chain (mtETC) complex III and this collapses the H^+ gradient across the mitochondrial inner membrane, resulting in disrupted ATP synthesis. Only in the absence of glucose or glycolysis, the parasites will derive ATP primarily from glutaminolysis driven mitochondrial oxidative phosphorylation, which will be susceptible to inhibition by atovaquone. As expected, we found that ATP synthesis in *wt* parasites, in the presence of glucose, was not inhibited by atovaquone. However, in the absence of glucose, glutamine-dependent ATP synthesis was completely inhibited by 200 nM atovaquone in *wt* parasites (Fig. 6C). This finding indicates that *T. gondii* tachyzoites are fully dependent on oxidative phosphorylation for ATP synthesis in the absence of glycolysis. In agreement with this finding, ATP synthesis in *Δhk* parasites was sensitive to atovaquone even in the presence of glucose (Fig. 6D), and complemented *Δhk*$^{+Tghk}$ parasite resembled wild type parasites in their response to atovaquone treatment (Supplementary Fig. S4B). ATP synthesis in *Δpepck1* parasites, under the different test conditions was similar to that observed with *wt* parasites (Supplementary Fig. S11).

4. Discussion

As an obligate intracellular parasite, *T. gondii* is dependent on host-derived glucose and glutamine for survival. Glucose metabolism is well studied in tachyzoite stage *T. gondii*, where a robust glycolytic flux is the major source of carbon and energy (ATP) for the parasite (Saliba and Kirk, 2001; Al-Anouti et al., 2004; MacRae et al., 2012). Although glucose is needed for optimal growth of *T. gondii*, it is not an essential nutrient. This was originally shown in studies using mutant parasites deficient in the major glucose transporter (*Δgt1*), where glutaminolysis was found to support growth of tachyzoite stage parasites (Blume et al., 2009). Moreover, genetic mutants of the glycolytic enzyme fructose 1,6 bisphosphate aldolase were viable, but only in the absence of glucose (Shen and Sibley, 2014). To further validate the essentiality of glycolysis in *T. gondii*, and to determine its role for asexual development of the parasite, we generated mutant parasites deficient in glycolysis by knocking out the gene coding for hexokinase (*Δhk*), which catalysis the first step in glycolysis.

Phenotypic studies with *wt* and *Δhk* parasites revealed that glucose is required for optimal growth and robust replication of tachyzoite stage parasites, and glutamine and other carbon sources such as acetate, succinate, pyruvate, glycerol and propionate cannot compensate for the fitness defect (Supplementary Fig. S1). This is intriguing since the fitness defect in glucose transporter (*Δgt1*) mutants was overcome by acetate supplementation. Scavenged acetate was primarily incorporated into lipid biomass, suggesting that the fitness defect in *Δgt1* parasites was primarily due to lipid biomass deficiency (Nitzsche et al., 2016). In *Δgt1* parasites, residual glycolytic activity is detectable, suggesting low levels of glucose entry into these cells. In contrast, we found that acetate supplementation was unable to overcome the fitness defect of *Δhk* parasites, likely due to that fact that these parasites are completely deficient in glucose oxidation via glycolysis, as seen in our metabolic labelling studies. This was further confirmed by plaque forming assays on *Δhk* mutants, with and without acetate supplementation (Supplementary Fig. S9B).

During asexual development, tachyzoite stage parasites convert to bradyzoites, which are responsible for the formation of tissue cysts in chronic infections (Dubey et al., 1998). Bradyzoites are slow growing forms and probably are less metabolically active than tachyzoites (Lunghi et al., 2015). Until now the role of glycolysis for bradyzoite formation was not studied. Here, we show that virulence associated with acute infection and mature tissue cyst formation during chronic infection is compromised in Type II Pru *Δhk* parasites (Fig. 2). These results suggest that for effective in vivo pathogenesis in a mammalian host, *T. gondii* requires glycolysis. Diminished tissue cyst formation in vivo, however, was not due to defective cyst wall polysaccharide synthesis, since Pru *Δhk* parasites were capable of differentiating into bradyzoites in vitro, and exhibited apparently normal cyst wall staining with *Dolichos biflorus* lectin. As shown for tachyzoite stage parasites, glutamine alone as a nutrient appears to be sufficient for in vitro bradyzoite formation by *T. gondii*. Therefore the inability of these parasites to form mature bradyzoite tissue cysts in vivo might be due to insufficient availability of glutamine. This is supported by our observation that host cell invasion and plaquing efficiency were greatly diminished in *Δhk* parasites in the absence of glutamine (Fig. 4B, C).

The metabolic changes in *Δhk* parasites were tracked using ^{13}C labelling studies. In contrast to *wt* parasites, in *Δhk* parasites there was a complete absence of glucose-derived ^{13}C labelling in intermediates of glycolysis, pentose phosphate pathway and Kreb's cycle. U^{13}C-U^{15}N-glutamine derived labelling patterns revealed that *Δhk* parasites generate glycolytic and pentose phosphate pathway intermediates via gluconeogenesis (Fig. 3, Supplementary Fig. S5). Only in *Δhk* parasites did we observe the formation of glutamine derived +3^{13}C- isotopomers for aspartate, malate and succinate, in addition to the +4^{13}C- isotopomers. This indicates that +3^{13}C-PEP, formed via the PEPCK reaction, is sequentially converted into +3^{13}C-pyruvate and +3^{13}C-oxaloacetate, which then equilibrates with aspartate, malate and succinate pools. Moreover, the formation of glutamine derived U^{13}C- and +5^{13}C- isotopomers of citrate, in addition to the +4^{13}C- isotopomer, indicates the BCKDH mediated formation +2^{13}C-acetyl-CoA as previously reported (Oppenheim et al., 2014). Taken together, our results from metabolic labelling studies with *Δhk* parasites are in agreement with that previously reported for the glucose transporter mutants (Nitzsche et al., 2016), and validates the importance of glutaminolysis and gluconeogenesis for survival of *T. gondii* in the absence of glycolysis.

Surprisingly, despite its importance, glutamine deprivation was not lethal for intracellular survival of *Δhk* parasites, although their fitness was greatly reduced (Fig. 4A). It is likely that glutamine-deprived intracellular *Δhk* parasites scavenge glutamine/glutamate from within host cells. Also, *Δpepck1* parasites, which are deficient in gluconeogenesis, failed to grow and replicate within host cells in the absence of glucose, suggesting that glutaminolysis-derived gluconeogenesis is the only mechanism by which *T. gondii* tachyzoites can assimilate carbon in the absence of glycolysis. To find out whether *Tgpepck1* is essential for asexual differentiation of tachyzoites to bradyzoites, we attempted to disrupt the *Tgpepck1* gene from the Pru strain (Type II) of *T. gondii*, but failed to obtain the mutants despite repeated attempts using either gene replacement or CRISPR/Cas9-mediated gene editing using two different guide RNAs. While the essentiality of the PEPCK enzyme in Pru strain *T. gondii* needs to be explored further, we found no difference whatsoever between *wt* RH and *wt* Pru strains in metabolic labelling experiments with glucose and glutamine. Interestingly, fructose-1,6 bisphosphatase (*Tgfbp2*), which catalyses the second reaction in gluconeogenesis, is essential for *T. gondii*, even in glucose replete conditions (Blume et al., 2015) and appears to mediate a futile cycle which regulates fructose-1,6 bisphosphate levels and carbon supply for synthesis of N-glycans, GPI anchor and amylopectin.

In contrast to intracellular *Δhk* parasites, when extracellular *Δhk* parasites are deprived of glutamine, they are greatly impaired in their ability to invade host cells and lose viability as observed in plaque forming assays (Fig. 4C). This is likely due to loss of ATP

synthesis, as confirmed by our experiments with atovaquone, which inhibits oxidative phosphorylation (McFadden et al., 2000). *Toxoplasma gondii* tachyzoites are capable of obtaining all of their ATP from either glycolysis or oxidative phosphorylation, and prior biochemical evidence suggests active mitochondrial oxidative phosphorylation in tachyzoites (Vercesi et al., 1998). In *wt* and *Δpepck1* parasites, atovaquone had no effect on ATP synthesis in the presence of glucose, in agreement with previous findings (Pomel et al., 2008). However, since oxidative phosphorylation is the only source of ATP for *Δhk* parasites, atovaquone completely abolished ATP synthesis in this parasite, even in the presence of glucose (Fig. 6). Overall, our findings suggest that *T. gondii* tachyzoite harbour a highly dynamic and essential mitochondrial oxidative metabolism, which can support parasite growth and differentiation in varying nutrient conditions. Further exploring the role of glycolysis and glutaminolysis in carbon and energy metabolism in the latent bradyzoite stages will help to reveal the metabolic requirements for tissue cyst formation and host persistence of this promiscuous parasite.

Acknowledgements

D.S. acknowledges funding from Ramalingaswami Re-Entry Fellowship, Department of Biotechnology, India (BT/RLF/Re-entry/53/2011) and CSIR-NCL, Pune (MLP026426); A.S. acknowledges Ph.D. fellowship from Indian Council of Medical Research, India (3/1/3/JRF-2011/HRD-149); M.L. acknowledges the Burroughs Welcome Fund Investigators in Pathogenesis of Infectious Disease (PATH) Award (1007041), USA, NIH Director's New Innovators award (1DP2OD001315-01), USA, and funding from the Center for Quantitative Biology (P50 GM071508), NIH, USA. The authors declare that they have no conflict of interest, financial or otherwise, pertaining to this study.

Appendix A. Supplementary data

Supplementary data associated with this article can be found, in the online version, at https://doi.org/10.1016/j.ijpara.2018.05.013.

References

Abdelbaset, A.E., Fox, B.A., Karram, M.H., Abd Ellah, M.R., Bzik, D.J., Igarashi, M., 2017. Lactate dehydrogenase in *Toxoplasma gondii* controls virulence, bradyzoite differentiation, and chronic infection. PLoS ONE 12, e0173745.

Al-Anouti, F., Tomavo, S., Parmley, S., Ananvoranich, S., 2004. The expression of lactate dehydrogenase is important for the cell cycle of *Toxoplasma gondii*. J. Biol. Chem. 279, 52300–52311.

Bahl, A., Davis, P.H., Behnke, M., Dzierszinski, F., Jagalur, M., Chen, F., Shanmugam, D., White, M.W., Kulp, D., Roos, D.S., 2010. A novel multifunctional oligonucleotide microarray for *Toxoplasma gondii*. BMC Genomics 11, 603.

Barban, S., 1962. Studies on the mechanism of resistance to 2-deoxy-D-glucose in mammalian cell cultures. J. Biol. Chem. 237, 291–295.

Blume, M., Rodriguez-Contreras, D., Landfear, S., Fleige, T., Soldati-Favre, D., Lucius, R., Gupta, N., 2009. Host-derived glucose and its transporter in the obligate intracellular pathogen *Toxoplasma gondii* are dispensable by glutaminolysis. PNAS 106, 12998–13003.

Blume, M., Nitzsche, R., Sternberg, U., Gerlic, M., Masters, S.L., Gupta, N., McConville, M.J., 2015. *Toxoplasma gondii* gluconeogenic enzyme contributes to robust central carbon metabolism and is essential for replication and virulence. Cell Host Microbe 18 (2), 210–220.

Bohne, W., Hunter, C.A., White, M.W., Ferguson, D.J., Gross, U., Roos, D.S., 1998. Targeted disruption of the bradyzoite-specific gene BAG1 does not prevent tissue cyst formation in Toxoplasma gondii. Mol. Biochem. Parasitol. 92, 291–301.

Boothroyd, J.C., Black, M., Bonnefoy, S., Hehl, A., Knoll, L.J., Manger, I.D., Ortega-Barria, E., Tomavo, S., 1997. Genetic and biochemical analysis of development in *Toxoplasma gondii*. Philos. Trans. R. Soc. Lond. B Biol. Sci. 352, 1347–1354.

Brayton, K.A., Lau, A.O., Herndon, D.R., Hannick, L., Kappmeyer, L.S., Berens, S.J., et al., 2007. Genome sequence of *Babesia bovis* and comparative analysis of apicomplexan hemoprotozoa. PLoS Pathog. 3, 1401–1413.

Chambers, M.C., Maclean, B., Burke, R., Amodei, D., Ruderman, D.L., et al., 2012. A cross-platform toolkit for mass spectrometry and proteomics. Nat. Biotechnol. 30, 918–920.

Clasquin, M.F., Melamud, E., Rabinowitz, J.D., 2012. LC–MS data processing with MAVEN: a metabolomic analysis and visualization engine. Curr Protoc. Bioinformatics, 11. Chapter 14 Unit14.

Crawford, M.J., Thomsen-Zieger, N., Ray, M., Schachtner, J., Roos, D.S., Seeber, F., 2006. *Toxoplasma gondii* scavenges host-derived lipoic acid despite its de novo synthesis in the apicoplast. EMBO J. 25, 3214–3222.

Donald, R.G., Carter, D., Ullman, B., Roos, D.S., 1996. Insertional tagging, cloning, and expression of the *Toxoplasma gondii* hypoxanthine-xanthine-guanine phosphoribosyltransferase gene. Use as a selectable marker for stable transformation. J. Biol. Chem. 271, 14010–14019.

Dubey, J.P., 1997. Bradyzoite-induced murine toxoplasmosis: stage conversion, pathogenesis, and tissue cyst formation in mice fed bradyzoites of different strains of *Toxoplasma gondii*. J. Eukaryot. Microbiol. 44, 592–602.

Dubey, J.P., Lindsay, D.S., Speer, C.A., 1998. Structures of *Toxoplasma gondii* tachyzoites, bradyzoites, and sporozoites and biology and development of tissue cysts. Clin. Microbiol. Rev. 11, 267–299.

Ferguson, D.J., Hutchison, W.M., 1987. An ultrastructural study of the early development and tissue cyst formation of *Toxoplasma gondii* in the brains of mice. Parasitol. Res. 73, 483–491.

Fleige, T., Fischer, K., Ferguson, D.J., Gross, U., Bohne, W., 2007. Carbohydrate metabolism in the *Toxoplasma gondii* apicoplast: localization of three glycolytic isoenzymes, the single pyruvate dehydrogenase complex, and a plastid phosphate translocator. Eukaryot. Cell 6, 984–996.

Foth, B.J., Stimmler, L.M., Handman, E., Crabb, B.S., Hodder, A.N., McFadden, G.I., 2005. The malaria parasite *Plasmodium falciparum* has only one pyruvate dehydrogenase complex, which is located in the apicoplast. Mol. Microbiol. 55, 39–53.

Fox, B.A., Ristuccia, J.G., Gigley, J.P., Bzik, D.J., 2009. Efficient gene replacements in *Toxoplasma gondii* strains deficient for nonhomologous end joining. Eukaryot. Cell 8, 520–529.

Fox, B.A., Falla, A., Rommereim, L.M., Tomita, T., Gigley, J.P., Mercier, C., Cesbron-Delauw, M.F., Weiss, L.M., Bzik, D.J., 2011. Type II *Toxoplasma gondii* KU80 knockout strains enable functional analysis of genes required for cyst development and latent infection. Eukaryot. Cell 10, 1193–1206.

Gardner, M.J., Hall, N., Fung, E., White, O., Berriman, M., Hyman, R.W., et al., 2002. Genome sequence of the human malaria parasite *Plasmodium falciparum*. Nature 419, 498–511.

Knoll, L.J., Boothroyd, J.C., 1998. Isolation of developmentally regulated genes from *Toxoplasma gondii* by a gene trap with the positive and negative selectable marker hypoxanthine-xanthine-guanine phosphoribosyltransferase. Mol. Cell. Biol. 18, 807–814.

Köhler, S., Delwiche, C.F., Denny, P.W., Tilney, L.G., Webster, P., Wilson, R.J., Palmer, J.D., Roos, D.S., 1997. A plastid of probable green algal origin in Apicomplexan parasites. Science 275, 1485–1489.

Konrad, C., Wek, R.C., Sullivan Jr., W.J., 2011. A GCN2-like eukaryotic initiation factor 2 kinase increases the viability of extracellular *Toxoplasma gondii* parasites. Eukaryot. Cell 10, 1403–1412.

Lea, P.J., Miflin, B.J., 1975. Glutamate synthase in blue-green algae. Biochem. Soc. Trans. 3, 381–384.

Lin, S.S., Blume, M., von Ahsen, N., Gross, U., Bohne, W., 2011. Extracellular *Toxoplasma gondii* tachyzoites do not require carbon source uptake for ATP maintenance, gliding motility and invasion in the first hour of their extracellular life. Int. J. Parasitol. 41, 835–841.

Lu, W., Clasquin, M.F., Melamud, E., Amador-Noguez, D., Caudy, A.A., Rabinowitz, J. D., 2010. Metabolomic analysis via reversed-phase ion-pairing liquid chromatography coupled to a stand alone orbitrap mass spectrometer. Anal. Chem. 82, 3212–3221.

Lunghi, M., Galizi, R., Magini, A., Carruthers, V.B., Di Cristina, M., 2015. Expression of the glycolytic enzymes enolase and lactate dehydrogenase during the early phase of *Toxoplasma* differentiation is regulated by an intron retention mechanism. Mol. Microbiol. 96, 1159–1175.

MacRae, J.I., Sheiner, L., Nahid, A., Tonkin, C., Striepen, B., McConville, M.J., 2012. Mitochondrial metabolism of glucose and glutamine is required for intracellular growth of *Toxoplasma gondii*. Cell Host Microbe 12, 682–692.

Mather, M.W., Henry, K.W., Vaidya, A.B., 2007. Mitochondrial drug targets in apicomplexan parasites. Curr. Drug Targets 8, 49–60.

McFadden, G.I., Reith, M.E., Munholland, J., Lang-Unnasch, N., 1996. Plastid in human parasites. Nature 381, 482.

McFadden, D.C., Tomavo, S., Berry, E.A., Boothroyd, J.C., 2000. Characterization of cytochrome b from *Toxoplasma gondii* and Q(o) domain mutations as a mechanism of atovaquone-resistance. Mol. Biochem. Parasitol. 108 (1), 1–12.

Melamud, E., Vastag, L., Rabinowitz, J.D., 2010. Metabolomic analysis and visualization engine for LC–MS data. Anal. Chem. 82, 9818–9826.

Nitzsche, R., Zagoriy, V., Lucius, R., Gupta, N., 2016. Metabolic cooperation of glucose and glutamine is essential for the lytic cycle of obligate intracellular parasite *Toxoplasma gondii*. J. Biol. Chem. 291, 126–141.

Nitzsche, R., Günay-Esiyok, Ö., Tischer, M., Zagoriy, V., Gupta, N., 2017. A plant/fungal-type phosphoenolpyruvate carboxykinase located in the parasite mitochondrion ensures glucose-independent survival of *Toxoplasma gondii*. J. Biol. Chem. 292, 15225–15239.

Olszewski, K.L., Morrisey, J.M., Wilinski, D., Burns, J.M., Vaidya, A.B., Rabinowitz, J.D., Llinás, M., 2009. Host–parasite interactions revealed by *Plasmodium falciparum* metabolomics. Cell Host Microbe 5, 191–199.

Oppenheim, R.D., Creek, D.J., MacRae, J.I., Modrzynska, K.K., Pino, P., et al., 2014. BCKDH: the missing link in apicomplexan mitochondrial metabolism is

required for full virulence of *Toxoplasma gondii* and *Plasmodium berghei*. PLoS Pathog. 10, e1004263.
Polonais, V., Soldati-Favre, D., 2010. Versatility in the acquisition of energy and carbon sources by the Apicomplexa. Biol. Cell 102, 435–445.
Pomel, S., Luk, F.C., Beckers, C.J., 2008. Host cell egress and invasion induce marked relocations of glycolytic enzymes in *Toxoplasma gondii* tachyzoites. PLoS Pathog. 4, e1000188.
Ralph, S.A., van Dooren, G.G., Waller, R.F., Crawford, M.J., Fraunholz, M.J., Foth, B.J., Tonkin, C.J., Roos, D.S., McFadden, G.I., 2004. Tropical infectious diseases: metabolic maps and functions of the *Plasmodium falciparum* apicoplast. Nat. Rev. Microbiol. 2, 203–216.
Reid, A.J., Vermont, S.J., Cotton, J.A., Harris, D., Hill-Cawthorne, G.A., et al., 2012. Comparative genomics of the apicomplexan parasites *Toxoplasma gondii* and *Neospora caninum*: Coccidia differing in host range and transmission strategy. PLoS Pathog 8, e1002567.
Rommereim, L.M., Hortua Triana, M.A., Falla, A., Sanders, K.L., Guevara, R.B., Bzik, D. J., Fox, B.A., 2014. Genetic manipulation in Δku80 strains for functional genomic analysis of *Toxoplasma gondii*. J. Vis. Exp. 77, e50598.
Roos, D.S., Crawford, M.J., Donald, R.G., Fraunholz, M., Harb, O.S., He, C.Y., Kissinger, J.C., Shaw, M.K., Striepen, B., 2002. Mining the *Plasmodium* genome database to define organellar function: what does the apicoplast do? Philos. Trans. R. Soc. Lond. B Biol. Sci. 357, 35–46.
Roos, D.S., Donald, R.G., Morrissette, N.S., Moulton, A.L., 1994. Molecular tools for genetic dissection of the protozoan parasite *Toxoplasma gondii*. Methods Cell Biol. 45, 27–63.
Rowell, P., Enticitt, S., Stewart, W.D.P., 1977. Glutamine synthetase and Nitrogenase activity in the blue-green algae *Anabaena cylindrical*. N. Phytol. 79, 41–54.
Saliba, K.J., Kirk, K., 2001. Nutrient acquisition by intracellular apicomplexan parasites: staying in for dinner. Int. J. Parasitol. 31, 1321–1330.
Seeber, F., 2003. Biosynthetic pathways of plastid-derived organelles as potential drug targets against parasitic apicomplexa. Curr. Drug Targets Immune Endocr. Metabol. Disord. 3, 99–109.
Seeber, F., Soldati-Favre, D., 2010. Metabolic pathways in the apicoplast of apicomplexa. Int. Rev. Cell Mol. Biol. 281, 161–228.
Shen, B., Brown, K.M., Lee, T.D., Sibley, L.D., 2014. Efficient gene disruption in diverse strains of Toxoplasma gondii using CRISPR/CAS9. MBio 5, e01114–e1214.
Shen, B., Sibley, L.D., 2014. *Toxoplasma* aldolase is required for metabolism but dispensable for host-cell invasion. PNAS 111, 3567–3572.
Sidik, S.M., Hackett, C.G., Tran, F., Westwood, N.J., Lourido, S., 2014. Efficient genome engineering of *Toxoplasma gondii* using CRISPR/Cas9. PLoS One 9, e100450.
Tymoshenko, S., Oppenheim, R.D., Agren, R., Nielsen, J., Soldati-Favre, D., Hatzimanikatis, V., 2015. Metabolic needs and capabilities of *toxoplasma gondii* through combined computational and experimental analysis. PLoS Comput. Biol. 11, e1004261.
Ufermann, C.M., Müller, F., Frohnecke, N., Laue, M., Seeber, F., 2017. *Toxoplasma gondii* plaque assays revisited: Improvements for ultrastructural and quantitative evaluation of lytic parasite growth. Exp. Parasitol. 180, 19–26.
Vercesi, A.E., Rodrigues, C.O., Uyemura, S.A., Zhong, L., Moreno, S.N., 1998. Respiration and oxidative phosphorylation in the apicomplexan parasite *Toxoplasma gondii*. J. Biol. Chem. 273, 31040–31047.
Woo, Y.H., Ansari, H., Otto, T.D., Klinger, C.M., Kolisko, M., Michálek, J., et al., 2015. Chromerid genomes reveal the evolutionary path from photosynthetic algae to obligate intracellular parasites. Elife 4, e06974.